PHYSICAL REVIEW C VOLUME 25, NUMBER 1 JANUARY 1982

Number conserving shell model for even Ca, Ti, Cr, and Fe isotopes

Y. K. Gambhir,* S. Haq, and J. K. Suri
Indian Institute of Technology, Bombay-400 076, India
(Received 22 December 1980; revised manuscript received 19 May 1981)

The nuclear properties of the low lying states of even isotopes of Ca, Ti, Cr, and Fe are calculated in the framework of the broken pair approximation. The broken pair approximation configuration space for an even number of identical valence nucleons includes all the seniority (ν) two components while for nonidentical (even-even) valence nucleons, it contains all configurations with $\nu \leq 4$ except $\nu=4$ proton components and $\nu=4$ neutron components. The calculations have been carried out with a ^{40}Ca core using two different sets of realistic interaction matrix elements: (i) the set reported by Kuo and Brown and its modified version due to McGrory; and (ii) a set of Tabakin interaction matrix elements which includes the second order Born term and core polarization effects. The effect of the truncation of the valence space has been examined in detail. The calculated energy spectra, quadrupole moments for the first 2^+ states, and $E2$ transition rates, compare well with the corresponding shell model results (wherever available) as well as with the experiment.

[NUCLEAR STRUCTURE Shell model, number conserving shell model, broken pair approximation, energy spectra, $E2$ transition rates, quadrupole moment, Ca, Ti, Cr, and Fe even isotopes.]

I. INTRODUCTION

Right from the time the shell model (SM) was established as the most basic model in nuclear structure, the nuclei in the $2p$-$1f$ region have been the focus of attention for various theoretical investigations based on the practical assumption of a ^{40}Ca inert core within the domain of the shell model. The complexities arising due to the large number of valence particles outside the ^{40}Ca core have hindered most of such theoretical attempts. Only very recently some calculations in the framework of the projected Hartree-Fock (PHF),[1] band mixing, and the highly truncated shell model have been reported for some of the nuclei in this region. The earlier SM attempts have been confined either to the $f_{7/2}$ valence space[2] only, or to the $f_{7/2}$ space with a few configurations involving the $p_{3/2}$ state.[3] The most systematic SM analysis has been carried out for Ca isotopes by McGrory *et al.*[4] in the valence space $f_{7/2}^{n_1} p_{3/2}^{n_2} f_{5/2}^{n_3} p_{1/2}^{n_4}$ with $n_3+n_4 \leq 2$. In another SM calculation[5] for nuclei with $A \leq 44$, the $E2$ transition rates for $^{42-44}$Ca and ^{44}Ti have also been reported. Both these SM calculations[4,5] have used the original set of realistic Kuo-Brown[6] (KB) interaction matrix elements, derived from the Hamada-Johnston potential, and its modified version[4] (KBM) obtained by changing some of the original $T=1$ KB interaction matrix elements. No such systematic shell model anlaysis for other nuclei in this region has been reported so far. Even the PHF and the band-mixing calculations using the KB and KBM interaction matrix elements have been confined to some odd-odd and even-odd (odd-even) nuclei in this region. Therefore, it is unnecessary to stress the importance of a systematic investigation for other nuclei in this region. To carry out the structure calculations for these nuclei in practice is indeed a challenging task considering the prohibitively large dimensions of the configuration space involved. Therefore, as a first step in this direction, we have carried out systematic calculations for the even isotopes of Ca, Ti, Cr, and Fe within the framework of the number conserving shell model, viz., the broken pair approximation (BPA).[7-10] It has been shown[9] that the BPA has all the advantages and none of the drawbacks of the quasiparticle theory. In addition, the BPA has a one-to-one correspondence at every step with the shell model. In this sense, the BPA is an approximation to the shell model and an improvement over the number projected quasiparticle

method.

The BPA starts with the assumption that the ground state for p pairs of identical nucleons is built up by p times repeated application on the particle vacuum of a distributed pair operator $C_\dagger$. The coefficients of distribution appearing in $C_\dagger$ are determined by minimizing the Hamiltonian with respect to the assumed ground state. This form of the approximate ground state, first proposed by Mottelson,[11] has the same structure as that of the number projected ($2p$-particle component) BCS state. In contrast to the BCS method, the BPA ground state parameters (occupancy/nonoccupancy probabilities) are determined through a minimization procedure after the projection rather than before. The BPA model space for a system having an even number of identical nucleons is then constructed through the replacement of one of the distributed pair operators $C_\dagger$ in the assumed approximate ground state by an arbitrary two particle configuration $[A^\dagger(abJM)]$. This is termed as one-BPA. In the successive approximations, two or more $C_\dagger$ operators in the approximate ground state are replaced by an equal number of $A^\dagger$ operators. It is to be noted that when all the $C_\dagger$ operators are replaced by an equal number of $A^\dagger$ operators, the full shell model Hilbert space is obtained. This procedure, guided by the strong pairing nature of the two body interaction, is analogous to the seniority truncation scheme. The only difference is that in BPA the pair operators $[A^\dagger(aaoo)]$ of the seniority truncation scheme are replaced by the distributed pair operator $C_\dagger$. This, in fact, is responsible for the large reduction in the shell model Hilbert space achieved by the BPA. For even-even nuclei having both types of nucleon in the valence shells (i.e., the nonidentical case), the BPA basis states in the first approximatioon are obtained from the product of one-BPA proton and one-BPA neutron states treating proton and neutron operators as independent. These BPA basis states, in general, are not orthogonal and therefore an orthonormal set of states is to be constructed before setting up the Hamiltonian matrices. In the case of one-BPA, which is analogous to seniority two ($v \leq 2$) truncation, the number of orthonormal BPA states is equal to the number of two-particle shell model configurations. This implies that the maximum dimensionality in the case of one-BPA is equal to that of the two particle (identical) shell model problem, in contrast to the large dimensionality encountered in the seniority two truncation scheme. Moreover, this dimensionality in the BPA is independent of the actual number of valence particles under consideration. For the nonidentical case, the number of independent BPA states is always the same as that of the four-particle (i.e., 2 proton + 2 neutron) shell model irrespective of the number of valence nucleons.

This practical aspect of the BPA can be better appreciated after having a look at Table I. This table lists the maximum dimensionalities of the energy matrices for various states encountered in the BPA in the full p-f space as well as in $f_{7/2}$-$p_{3/2}$ space. The SM dimensionalities for 6, 8, and 12 valence particles ($T=1$ only)[12] are also included in this table to demonstrate the nontractable nature of the shell model calculations.

We have carried out the BPA calculations for even isotopes of Ca, Ti, Cr, and Fe, assuming ^{40}Ca as the inert core. In addition to the original set of Kuo-Brown matrix elements and its modified version, another appropriate set of Tabakin interaction matrix elements (TB) and its modified version TBM (the modification is similar to that used for obtaining KBM) have also been used in the present calculations. First, the BPA calculations for even Ca isotopes (i.e., the identical nucleon case) are performed in the full p-f space. The results compare very well with the SM results[4] and both

TABLE I. The dimensionalities of the shell model and the BPA Hamiltonian matrices for the valence nucleon number N ($N=4$, 6, 8, and 12) in the full and the truncated f-p space.

J	BPA		Shell model ($T=1$ only)		
$N\rightarrow$	4[a]	4[b]	6[a]	8[a]	12[a]
0	158	20	1514	17437	671159
2	596	62	6338	77907	3067868
4	655	72	8026	106132	4461696
6	423	53	6606	98092	4984885

[a]Full f-p space.
[b]$f_{7/2}$-$p_{3/2}$ space.

reproduce the observed systematics reasonably well. The BPA calculations are then repeated in the truncated space consisting of $f_{7/2}$ and $p_{3/2}$ states. The effective interaction matrix elements for the truncated space calculation are obtained through the projection method[13,14] which incorporates the effects of the valence space truncation. An excellent agreement observed between the results of the full and the corresponding truncated space calculations encourages us to perform further calculations in the truncated space only. This aspect is particularly useful for the nonidentical nucleon case where further reduction in the BPA configuration space is highly desirable from the computational point of view (cf. columns 2 and 3 of Table I). Therefore, the energy spectra and the electromagnetic transition rates for Ti, Cr, and Fe isotopes (i.e., the nonidentical nucleon case) are calculated in the truncated space alone. The BPA results reproduce reasonably well the observed level systematics and the transition rates. The SM results[5] are available only for ^{44}Ti; the BPA results for this nucleus are in good agreement with these SM results. The energy spectra and the electromagnetic transition rates for $N=28$ isotones (the identical nucleon case) have also been examined with respect to the ^{48}Ca core using an appropriate set of interaction matrix elements. The results indicate the importance of neutron excitations, especially for the high lying states.

The BPA formalism is briefly sketched in Sec. II. The details of the calculation and the results are presented and discussed in Sec. III. Section IV contains the concluding remarks.

II. BROKEN PAIR APPROXIMATION FORMALISM

A. Basis states

The BPA assumes that the ground state ϕ_0 for p pairs of identical particles is obtained by repeated (p times) application of a distributed pair operator $C_\dagger$ on the particle vacuum, i.e.,

$$\phi_0 \rightarrow C_\dagger^p \mid 0\rangle = \left[\sum_a \frac{v_a}{u_a}\frac{\bar{a}}{2} A^\dagger(aaoo)\right]^p \mid 0\rangle$$
$$\rightarrow \tau_p^\dagger \mid 0\rangle = \frac{1}{p!}\left[\prod_a u_a{}^{\bar{a}^2/2}\right] C_\dagger^p \mid 0\rangle \tag{2.1}$$

with $v_a{}^2+u_a{}^2=1$ and

$$A^\dagger(abJM)=\sum_{\alpha,\beta}\begin{bmatrix} a & b & J \\ \alpha & \beta & M\end{bmatrix} c_\alpha^\dagger c_\beta^\dagger .$$

Here "α" denotes a set of quantum numbers (n,l,j,m) required to specify a single particle state while the letter "a" represents only n,l,j quantum numbers. $c^\dagger(c)$ is a single particle fermion creation (annihilation) operator and $\bar{a}=(2j_a+1)^{1/2}$.

The ground state parameters $u(v)$ are obtained by minimizing the Hamiltonian, i.e.,

$$\delta\frac{\langle\phi_0 \mid H \mid \phi_0\rangle}{\langle\phi_0 \mid \phi_0\rangle}=0 . \tag{2.2}$$

It is to be noted that the structure of the approximate BPA ground state (2.1) is identical to that of the $2p$-particle component of the BCS state. In fact, these two states become identical when the ground state parameters $u(v)$ are replaced by the corresponding BCS quantities $U(V)$, i.e., nonoccupation (occupation) probabilities. It has been shown[7] that the projected BCS state has about 99% overlap with the seniority zero shell model ground state. Furthermore, the differences in the occupation probabilities obtained by the exact and approximate minimization of the (v_a/u_a) coefficients have been reported[15] to be small. This implies that the approximate BPA ground state is indeed very close to the true ground state and that the replacement of $u(v)$ by $U(V)$ is a good approximation.

The BPA basis states are constructed by replacing one $C_\dagger$ operator in the ground state ϕ_0 by an arbitrary two particle creation operator $A^\dagger(abJM)$. Therefore, the BPA basis states in this approximation (i.e., one-BPA) are given as

$$\mid \Psi(abJM)\rangle = A^\dagger(abJM)\tau_{p-1}^\dagger \mid 0\rangle . \tag{2.3}$$

The approximate ground state (2.1) is a linear combination of the states (2.3) with $J=0$. Therefore, it is sufficient to work with an orthonormal set of states constructed from the states (2.3). The number of independent one-BPA states is equal to that of two particle SM states and furthermore, this number in one-BPA remains unaltered irrespective of the actual number of valence nucleons present.

In the successive approximations the BPA basis states can be constructed by replacing more $C_\dagger$ operators by an equal number of $A^\dagger$ operators.

The states (2.3), in general, are not orthogonal and therefore need to be orthogonalized before using them for setting up the Hamiltonian matrices. The orthogonalization procedure requires the knowledge of the overlaps between the BPA states. The procedure for evaluating these overlaps is given in detail in Ref. 9.

For the nonidentical nucleon case, the ground state for even-even nuclei, having both types of nucleons in the valence shells, is expressed as a product of a proton paired (p pairs) state $\tau_p^\dagger|0\rangle$ and a neutron paired (n pairs) state $\tau_n^\dagger|0\rangle$, i.e.,

$$|\phi_0\rangle=[\tau_p^\dagger\otimes\ \tau_n^\dagger]|0\rangle\ . \tag{2.4}$$

The state (2.4) is valid especially for the cases where the valence protons and neutrons fill different major shells. The basis space is constructed by coupling proton and neutron wave functions, after proper replacement of a proton (and a neutron) distributed pair operator by a corresponding two particle creation operator $A^\dagger(abJM)$. The replacement of operator $C_\dagger$ is done in accordance with the procedure outlined for the identical nucleon system.

The BPA basis states in this case are then explicitly written as

$$\phi(a_1a_2J_\pi,b_1b_2J_\eta;JM)\rightarrow[\tau_{p-1}^\dagger A^\dagger(a_1a_2J_\pi)\otimes\ \tau_{n-1}^\dagger A^\dagger(b_1b_2J_\eta)]_M^J|0\rangle\ , \tag{2.5}$$

where a's represent protons, b's represent neutrons, and the symbols π and η are used for distinct identification of the proton and neutron systems, respectively.

For seniority zero, the state (2.4) is a particular linear combination of the states (2.5). Moreover, for $J_\pi=0$ (or $J_\eta=0$), the states (2.5) are not orthogonal. Therefore, it is sufficient to consider only the states (2.5) for constructing an orthonormal set of basis states following a procedure similar to that already described for the identical nucleon system. It is clear that the states (2.5) contain all the low seniority ($v=0,2,4$) components of the shell model wave functions except the $v=4$ proton components and the $v=4$ neutron components. Further, for the case of four valence particles (i.e., two protons and two neutrons), the states (2.5) become identical to the corresponding exact shell model states. Therefore, for such cases, both the BPA and the exact shell model calculations carried out with the same input information will produce identical results.

The most important feature of the present BPA formulation [cf. (2.5)] is that whatever the number of valence (even-even) nulceons is, the maximum dimensionality of the BPA Hamiltonian matrices is equal to the exact shell model dimensionality of a four-nucleon case (i.e., corresponding to 2 protons and 2 neutrons). This great reduction in the size of Hamiltonian matrices makes them tractable for numerical computation on the available modern computers and, therefore, paves the way for studying most of the nuclei for which the shell model calculations are just not feasible.

B. Matrix elements of Hamiltonian

The shell model Hamiltonian H for spherical nuclei can be written as

$$H=H_0+H_{\rm int}\ , \tag{2.6}$$

with

$$H_0=\sum_\alpha \epsilon_\alpha c_\alpha^\dagger c_\alpha\ , \tag{2.7}$$

and

$$H_{\rm int}=\tfrac{1}{4}\sum_{\alpha\beta\gamma\delta}\langle\alpha\beta|V|\gamma\delta\rangle_{\rm ex}c_\alpha^\dagger c_\beta^\dagger c_\delta c_\gamma\ . \tag{2.8}$$

Evaluation of the matrix elements of the Hamiltonian in BPA is greatly simplified if the Hamiltonian is rewritten in such a form that all the annihilation operators appear on the left and all the creation operators appear on the right. This can be achieved by using the anticommutation property of the fermion operators and treating the neutron and the proton operators as independent.

The Hamiltonian in its final form can be expressed as

$$H=H_{PP}+H_{NN}+H_{PN}\ . \tag{2.9}$$

The proton-proton part (H_{PP}) of the Hamiltonian consists of:

(i) an operator free term (i.e., a constant);
(ii) a term with an operator of the form $c_\alpha c_\alpha^\dagger$;
(iii) a term with an operator of the form $AA^\dagger$.

In the calculation of the matrix elements of H_{PP} between the BPA states, one is required to evaluate

$$\langle 0|\tau_{p-1}A(a_1'a_2'J_\pi'M_\pi')|O_{PP}|A^\dagger(a_1a_2J_\pi M_\pi)\tau_{p-1}^\dagger|0\rangle \tag{2.10}$$

with $O_{PP}=1$, $c_\alpha c_\alpha^\dagger$, and $AA^\dagger$, respectively.

The expressions (2.10) with different O_{PP} can be calculated by coupling the annihilation operator(s) $c(A)$ to the BPA state on the bra side and the creation operator(s) $c^\dagger(A^\dagger)$ to the BPA state on the ket side, resulting in new BPA states corresponding to $2p+1$ $(2p+2)$ particles both on bra and ket sides. Thus, the problem of evaluating the matrix elements of H reduces to the evaluation of the overlaps between the BPA states. The final expres-

sion for the matrix element of H involves these overlaps, the particle-particle matrix elements (G functions) and hole-particle matrix elements (F functions), and some geometrical factors. The one-BPA which will be referred to as "the BPA," the expression for the matrix element of H, can be further simplified and is given in Ref. 9.

Similarly, the matrix element of H_{NN} can easily be evaluated. In fact, the final expression for this case will be the same as that for H_{pp} with proton (neutron) suffixes replaced by neutron (proton) suffixes.

The H_{PN} part of the Hamiltonian in the rewritten form consists of a constant $H_{PN}^{(0)}$ and terms $H_{PN}^{(P)}$, $H_{PN}^{(N)}$, and H_{PN} involving the following operators:

(i) only proton operators: $c_{\pi}c_{\pi}^{\dagger}$;
(ii) only neutron operators: $c_{\eta}c_{\eta}^{\dagger}$;
(iii) mixed operators: $c_{\pi'}c_{\pi}^{\dagger}c_{\eta'}c_{\eta}^{\dagger}$, respectively.

The constant $H_{PN}^{(0)}$ contributes only to the diagonal matrix element. Since the proton and neutron operators are independent, the matrix element of the $H_{PN}^{(P)}$ involving only the single particle proton operator can be evaluated following the procedure adopted for the one body part of H_{pp}. The expression for the $H_{PN}^{(N)}$ part is the same as that of $H_{PN}^{(N)}$ with all the proton (neutron) suffixes replaced by the neutron (proton) suffixes. For the case of H_{PN}, where the mixed operators are invloved, the matrix element between the BPA states factors out as a product of

$$\langle 0 \,|\, \tau_{p-1} A(a_1' a_2' J_{\pi'} M_{\pi'}) \,|\, c_{\pi'} c_{\pi}^{\dagger} \,|\, A^{\dagger}(a_1 a_2 J_{\pi} M_{\pi}) \tau_{p-1}^{\dagger} \,|\, 0 \rangle$$

and

$$\langle 0 \,|\, \tau_{n-1} A(b_1' b_2' J_{\eta'} M_{\eta'}) \,|\, c_{\eta'} c_{\eta}^{\dagger} \,|\, A^{\dagger}(b_1 b_2 J_{\eta} M_{\eta}) \tau_{n-1}^{\dagger} \,|\, 0 \rangle \ .$$

These two terms of the product can be reduced to an overlap between the BPA proton states with $(2p+1)$ particles and between the BPA neutron states with $(2n+1)$ particles. The final expression for the matrix elements of H_{PN} between the BPA states is lengthy and therefore will not be presented here.

C. Electromagnetic transition rates and moments

The electromagnetic reduced transition probabilities and the static moments are simply related to the quantity

$$\langle J || \hat{O}^{\lambda} || J' \rangle \tag{2.11}$$

in which $|JM\rangle$ and $J'M'\rangle$ are the pertinent nuclear states, which in the present formalism are linear combinations of the BPA basis states (2.3). In order to simplify the evaluation of the reduced matrix elements (defined as in Ref. 16) of $\hat{O}_{\mu}^{\lambda}$, it is expressed in a form in which the particle annihilation operators appear on the left and the particle creation operators appear on the right. For $\lambda \neq 0$, the reduced matrix elements between the BPA states (2.3) can be written as

$$\begin{aligned}\langle \tau_{p-b} A(a_1' a_2' J') || \hat{O}^{\lambda} || A^{\dagger}(a_1 a_2 J) \tau_{p-b}^{\dagger} \rangle &= \sum_{a,a'} \langle a || \hat{O}^{\lambda} || a' \rangle \sum_{j} (-1)^{J-a-j} \bar{J}^2 W(JJ'aa';\lambda j) \\ &\times \langle 0 \,|\, [[c_{a'}^{\dagger} \otimes A^{\dagger}(a_1' a_2' J')]^{j}]^{\dagger} \tau_{p-b} \tau_{p-b}^{\dagger} [c_a^{\dagger} \otimes A^{\dagger}(a_1 a_2 J)]^{j} \,|\, 0 \rangle \ . \end{aligned} \tag{2.12}$$

Since Eq. (2.12) involves the overlaps between the BPA states, the reduced matrix elements of the electromagnetic transition operator can be evaluated following a procedure similar to that used for the Hamiltonian matrices. The final expression for the reduced matrix elements, suitable for numerical computation, is given in Ref. 9.

For the nonidentical case, the BPA wave function can be expressed as a linear combination of the states $|\Phi(a_1 a_2 J_{\pi}, b_1 b_2 J_{\eta}; JM\rangle$ with the expansion coefficients obtained by diagonalizing the BPA energy matrices. The calculation of the electromagnetic transition rates, etc., will thus involve the evaluation of the reduced matrix elements

$$\langle \Phi(a_1' a_2' J_\pi', b_1' b_2' J_\eta'; J') || \hat{O}^\lambda || \Phi(a_1 a_2 J_\pi, b_1 b_2 J_\eta; J) \rangle \ . \tag{2.13}$$

The electromagnetic transition operator $\hat{O}_\mu^\lambda$ is a one body operator and at a time it can affect either a proton state or a neutron state. Therefore, the proton (or neutron) part can be factored out which can be expressed as an overlap between the BPA states for protons (or neutrons).

Thus the proton part of the reduced matrix elements between the BPA states for nonidentical case can be expressed in terms of the reduced matrix elements between the proton BPA states together with an overlap between the neutron BPA states and some geometrical factors. An identical procedure can be followed for the evaluation of the neutron part of the operator. In fact, the expression for the neutron part will be the same as that for the proton part with all the proton suffixes $p(n)$ replaced by the corresponding neutron suffixes $n(p)$. This makes the formulation comparatively easier.

It is to be stressed that the BPA technique, discussed above for evaluating the matrix elements of various operators, is quite general and therefore can be used for the calculation of various physical quantities like spectroscopic amplitudes (for one- and two-nucleon transfer reactions), β-decay matrix elements, etc. The final expression for the matrix elements of such physical operators, in BPA, can always be reduced to a form involving overlaps between the BPA states which is ideally suitable for numerical computation.

III. CALCULATIONS, RESULTS, AND DISCUSSION

Explicit calculations have been performed for the even isotopes of Ca, Ti, Cr, and Fe. The single particle level energies (SPE) and the two body matrix elements relevant to the valence space under consideration form an essential part of the input data. In the present calculation, two sets of SP energies have been tried along with the following sets of the realistic interaction matrix elements:

(i) the original Kuo-Brown[6] set of two body interaction matrix elements, with respect to the ^{40}Ca core, obtained from the free nucleon-nucleon Hamada-Johnston[17] potential. This set has also been used frequently in earlier structure calculations. McGrory *et al.*,[4] in order to improve the overall agreement in their SM calculations for $^{42-50}$Ca, have modified some of the $T=1$ original KB matrix elements by the least squares fitting procedure. The modifications introduced in the $\langle f_{7/2} j J, T=1 \mid V \mid f_{7/2} j J, T=1 \rangle$ matrix elements are (a) -0.3 MeV for $j=f_{7/2}$, $+0.3$ MeV for $j=p_{3/2}$ (both for $J=0$ and 2); and (b) $+0.25$ MeV for $j=p_{1/2}, f_{5/2}$ for all permitted J. This modified set of KB matrix elements has also been used in the present calculation.

(ii) the set of Tabakin interaction matrix elements,[18] appropriate to this region, derived from the nonlocal separable potential of Tabakin.[19] In this set the second order Born term, which has been shown to be important by Kerman and Pal,[20] has been included in the second order perturbation theory using the plane wave intermediate states and an angle averaged Pauli operator. In order to make this second order Born term independent of the center of mass radial node quantum number, an averaging procedure similar to that of Clement and Baranger[21] has been adopted. In addition, the core contributions with 3p-1h intermediate states are also incorporated in the perturbation theory. For this purpose, the following five hole states and nine particle states are considered:

	Hole states (energy in MeV)				
$1p_{3/2}$ (−20.0)	$1p_{1/2}$ (−20.0)	$1d_{5/2}$ (−10.0)	$2s_{1/2}$ (−10.0)	$1d_{3/2}$ (−10.0)	
	Particle states (energy in MeV)				
Valence:	$1f_{7/2}$ (−5.0)	$2p_{3/2}$ (0.0)	$1f_{5/2}$ (0.78)	$2p_{1/2}$ (1.08)	
High lying:	$1g_{9/2}$ (3.5)	$2d_{5/2}$ (10.0)	$1g_{7/2}$ (10.0)	$3s_{1/2}$ (10.0)	$2d_{3/2}$ (10.0)

This set of Tabakin interaction matrix elements obtained here is denoted by TB and its modified version by TBM (modifications in the selected $T=1$ matrix elements identical to those used for obtaining KBM from KB). Both TB and TBM have been used in the present work. We performed the BPA calculations for $^{42-46}$Ca with respect to the ^{40}Ca inert core, using the Tabakin interaction matrix elements, with the experimental[22] as well as with the Kuo-Brown SPE.[6] The results reveal that the spectra obtained by using two sets of SPE are quite close, indicating thereby that either set can be used in the calculation with almost the same degree of reliability. Therefore, in order to maintain consistency in the calculations and to facilitate the comparison with the available shell model calculations, we use the Kuo-Brown SPE throughout in the present investigation.

As most of the earlier shell model calculations in the $2p$-$1f$ region have been carried out in highly truncated space(s), or only a restricted number of the p-f configurations have been included in the model space, therefore the BPA calculations in similar spaces have also been carried out using the appropriately renormalized two body matrix elements obtained by the projection method.[13,14]

The labels used to designate the results of our calculations in various spaces, using different effective interactions, are summarized in Table II. The labels used to identify the shell model results of McGrory *et al.*[4] for Ca isotopes, often referred to in the present work, are also included in the same table. All experimental values will be designated by the label expt. It is observed that the BPA results obtained with the Tabakin interaction matrix elements are very similar to those obtained with the corresponding Kuo-Brown interaction matrix elements. In other words, the TB, TBT I, and MTB sets of results are very close to those of KB, KBT I, and MKB, respectively. Therefore, we present and discuss only the BPA results obtained by using the Tabakin interaction matrix elements; however, all the remarks made for these results do apply to the corresponding sets of results of the Kuo-Brown interaction matrix elements.

The lowest three BPA energy values for each of the positive-parity, even-spin states ($0^+,2^+,4^+,6^+$) are presented in various figures. The corresponding shell model levels as well as the observed levels are also shown in these figures for comparison. If an excited state does not appear even once in the low lying spectra, its position is numerically indicated in the level diagrams, above the break shown in the usual energy scale. Since the first excited state in the observed spectrum of ^{48}Ca appears at 3.83 MeV and all the other states lie above 4.0 MeV, we have extended the energy scale (Fig. 4) to 6.0 MeV for this isotope.

In the various figures the results are presented in a form in which the calculated 2^+ level is made to coincide with the observed 2^+ state (i.e., by introducing an appropriate "shift" in the calculated levels). This shift is numerically indicated in the ground state in all the level diagrams (see e.g., Figs. 1—5 for Ca isotopes). Similar scaling has also been used by Bhatt and McGrory.[27].

A. Energy spectra

1. *Calcium isotopes*

The BPA results for Ca isotopes are plotted in Figs. 1—5. We do not intend to remark on every aspect of the calculated results for each of the lev-

TABLE II. The labels used to designate the results of the BPA calculations performed in different spaces using different interaction matrix elements along with the labels used for designating the shell model (SM) results for Ca isotopes of Ref. 4.

	Full space		Truncated space I	Truncated space II
	SP orbits: $f_{7/2}p_{3/2}f_{5/2}p_{1/2}$		$f_{7/2}p_{3/2}$	$f_{7/2}$
Interaction	BPA	SM	BPA	BPA
Tabakin	TB		TBT I	TBT II
Kuo-Brown	KB	MG (fp)	KBT I	
Modified ($T=1$) Tabakin	MTB		MTBT I	
Modified ($T=1$) Kuo Brown	MKB	MG (fp')		

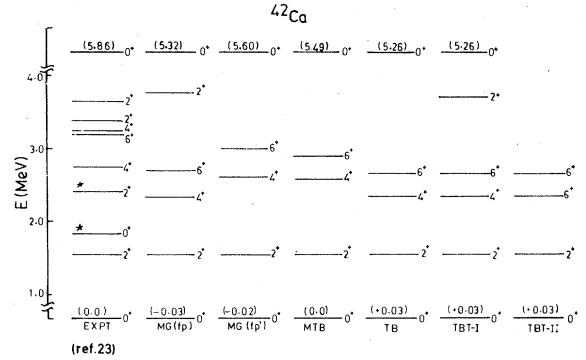

FIG. 1. The experimental (expt), the shell model, and the BPA energy spectra for ^{42}Ca plotted by matching the calculated 2_1^+ state with the experimental 2_1^+ state. The resulting shift is numerically indicated in the parentheses just above the ground state in each spectrum. Any first excited state not appearing up to 4 MeV is also indicated numerically above the broken scale. The labels representing various calculated spectra are explained in Table II. Asterisk is used for showing core-excited states in the experimental spectrum.

els; instead we prefer to leave the results to speak for themselves. It is observed that the low lying states in the full f-p space are mostly in good agreement with the corresponding shell model [MG (fp)] as well as with the experimental (expt) levels. The first excited 0^+ and the second excited 2^+ states for ^{42}Ca and ^{44}Ca are not reproduced by the BPA. These states are also not reproduced by the shell model calculations. In fact, these states have been attributed[2,4] to core excited configurations not included in the f-p space. The use of the modified matrix elements does improve the results slightly for ^{48}Ca and ^{50}Ca. For ^{48}Ca the low lying states do appear in our calculation as well as in the shell model calculation of McGrory *et al.*[4] [MG

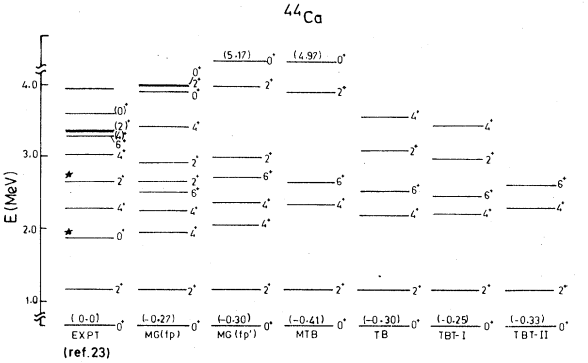

FIG. 2. The experimental (expt), the shell model, and the BPA energy spectra with shift for ^{44}Ca. For details see caption for Fig. 1.

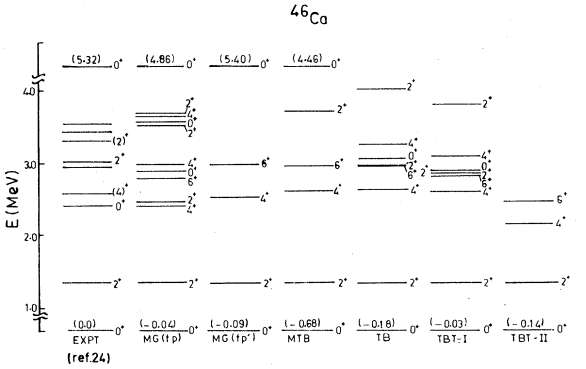

FIG. 3. The experimental, the shell model, and the BPA energy spectra with shift for ^{46}Ca. For details see caption for Fig. 1.

(fp)]. This may be due to the fact that the Tabakin and the Kuo-Brown matrix elements may not account for the $f_{7/2}$ shell closure. However, the modifications in the interaction matrix elements, which presumably take care of this $f_{7/2}$ shell closure in the shell model [Mg (fp')], help to push up the calculated levels significantly. Our results MTB and MKB, too, show a similar trend. The BPA results for ^{50}Ca are not as satisfactory as for the other isotopes of Ca. Even the corresponding shell model calculations exhibit a trend similar to ours.

It is found that most of low lying states are well reproduced even in the truncated space calculations except for the TBT II levels of ^{46}Ca which are slightly pushed down. This is not surprising because the only valence shell ($f_{7/2}$) in the TBT II space is nearing closure.

The present analysis of Ca isotopes therefore reveals that the BPA results are very similar to the

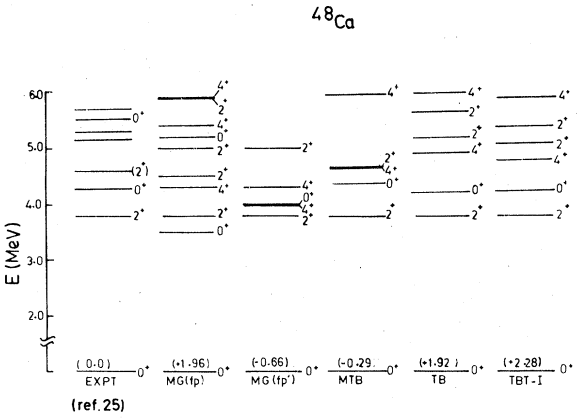

FIG. 4. The experimental (expt), the shell model, and the BPA energy spectra with shift for ^{48}Ca. For details see caption for Fig. 1.

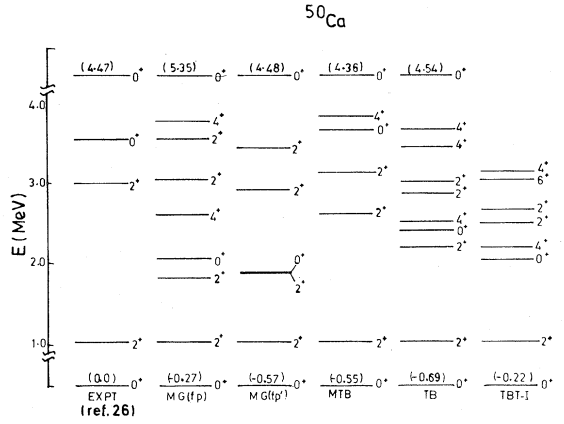

FIG. 5. The experimental, the shell model, and the BPA energy spectra with shift for ^{50}Ca. For details see caption for Fig. 1.

corresponding shell model results and that both reproduce the experimental trends equally well. This demonstrates that the BPA, which in comparison to the conventional shell model, requires much less labor in practice (due to a great reduction in dimensionalities of the Hamiltonian matrices), can be considered a reliable, successful, and practical approximation to the shell model in this region. It is further revealed that the projection method successfully incorporates the effects of space truncation through the renormalization of the interaction matrix elements. Therefore, the calculations in the truncated space can be performed with confidence by using the renormalized matrix elements obtained by the projection method.

2. *N*=28 Isotones

The main intention behind the present analysis of the $N=28$ isotones (^{50}Ti, ^{52}Cr, ^{54}Fe) in the framework of the BPA is to exhibit the shell closure effects at $N=28$ and to study the usefulness of ^{48}Ca as an inert core in the f-p shell.

Energy spectra of ^{50}Ti, ^{52}Cr, and ^{54}Fe. The BPA calculations are carried out for ^{50}Ti, ^{52}Cr, and ^{54}Fe assuming ^{48}Ca as an inert core. All the four valence proton orbitals $f_{7/2}$, $p_{3/2}$, $f_{5/2}$, and $p_{1/2}$ are considered in the model space. The relevant Kuo-Brown SPE of these orbitals, used in the calculation, are listed below. An appropriate set of the $T=1$ two body matrix elements with respect to the ^{48}Ca core obtained[18] from the nonlocal separable potential of Tabakin[19] is employed in the calculation.

Proton orbital:	$f_{7/2}$	$p_{3/2}$	$f_{5/2}$	$p_{1/2}$
Kuo-Brown SPE (MeV):	0.0	4.4	6.9	5.9

The BPA results (TB) and the corresponding experimental values (expt) are presented in Fig. 6.

These results clearly indicate that the first excited state for each spin (2^+,4^+,6^+) is reproduced reasonably well, while the other excited states lie very high compared to the experiment. Figure 6 shows that few levels around 3 MeV appearing in the observed spectra (expt) of ^{52}Cr and ^{54}Fe are not reproduced by the BPA calculation. This indicates that only the proton excitations considered in the BPA calculation are not sufficient to explain the observed spectra of these isotones. The neutron excitations, neglected by the assumption of a ^{48}Ca inert core, seem to play an important role, and therefore these should be included in the calculation for an accurate description of the nuclear properties in this region.

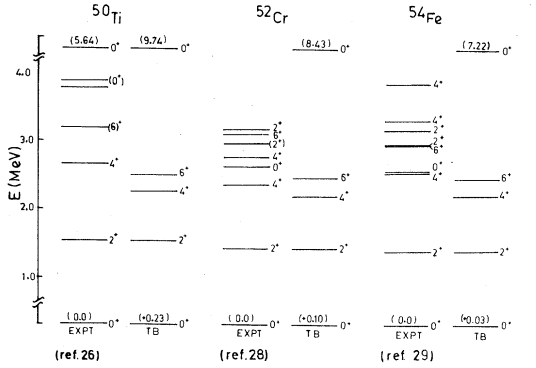

FIG. 6. The experimental (expt) and the BPA energy spectra with shift for $N=28$ isotones in the full f-p space w.r.t. ^{48}Ca core.

B. *E*2 transitions and quadrupole moments

1. Calcium isotopes

The calculated $B(E2)$ values for Ca isotopes are presented in Table III. The labels TB and TBT I correspond to the results in full and truncated spaces, respectively. The $Q_{2_1^+}$ values are plotted in

TABLE III. The calculated, the shell model (SM), and the experimental (expt) $B(E2{:}J_i \rightarrow J_f)$ for even Ca isotopes.

Nucleus	Transition $j_f \rightarrow J_f$	$B(E2)$ $(e^2\,\mathrm{fm}^4)$ TB[a]	TBT I[a]	SM[b]	expt	Reference[c]
^{42}Ca	$2_1^+ \rightarrow 0_{g.s.}^+$	27.4	27.1	26	81.5 ± 3.0	30
	$4_1^+ \rightarrow 2_1^+$	28.3	26.6	27	57.5 ± 4.5	30
	$6_1^+ \rightarrow 4_1^+$	15.4	15.3	14	6.44± 0.19	30
^{44}Ca	$2_1^+ \rightarrow 0_{g.s.}^+$	47.9	45.3	42	100 ±6	30
	$4_1^+ \rightarrow 2_1^+$	2.6	1.5	20	75 ±15	31
					160 ±60	31
	$6_1^+ \rightarrow 4_1^+$	0.7	0.4	8	41.2 ± 3.6	30
					50 ±12	31
^{46}Ca	$2_1^+ \rightarrow 0_{g.s.}^+$	58.2	52.3		35.1 ±3.6	30
	$4_1^+ \rightarrow 2_1^+$	2.1	4.6			
	$6_1^+ \rightarrow 4_1^+$	3.4	5.0		5.34± 0.28	30
^{48}Ca	$2_2^+ \rightarrow 0_{g.s.}^+$	64.0				
^{50}Ca	$2_1^+ \rightarrow 0_{g.s.}^+$	59.3				

[a] $e_n^{\mathrm{eff}} = 1.0e$.
[b] Reference 5, $e_n^{\mathrm{eff}} = 1.0e$.
[c] Reference to experimental data.

Fig. 7. The corresponding experimental values, wherever available, are also included in the tables. References to the experimental data are also indicated there.

The shell model $B(E2)$ values for the electromagnetic transitions in Ca isotopes have been reported by McGrory[5] only for ^{42,44}Ca. These are also included in Table III for comparison, in the column labeled SM. Although the shell model wave functions for heavier isotopes of Ca are available,[4] the transition rates, etc., for these isotopes have not been reported so far.

Table III shows that most of the calculated (TB and TBT I) $B(E2)$ values for Ca isotopes are in good agreement with the corresponding SM values, and both reproduce the experimental trend reasonably well. A proper choice of neutron effective charge ($\sim 1.5e$) will lead to an overall good agreement with the experiment.

The calculated $B(E2{:}2_1^+ \rightarrow 0_{g.s.}^+)$ values for all the Ca isotopes with $e_n^{\mathrm{eff}} = 1.0e$ are plotted (TB) in Fig. 8 along with the experimental values. Just to have an idea as to how the agreement can be improved by choosing the proper nucleon effective charge, the TBT I results obtained in the truncated space calculation are plotted (Fig. 8) with $e_n^{\mathrm{eff}} = 1.5e$ (TBT I[b]) along with the corresponding results with $e_n^{\mathrm{eff}} = 1.0e$ (TBT I[a]).

It is revealed in Fig. 8 that the TB and TBT I[a] curves, corresponding to the same effective charge $1.0e$, are very similar. The calculated

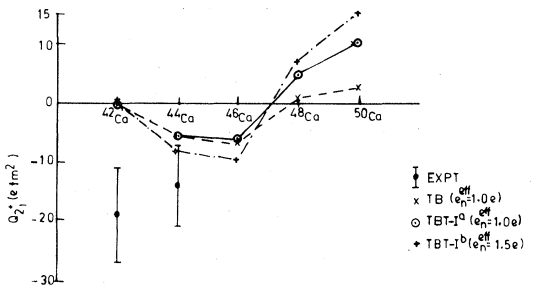

FIG. 7. The quadrupole moment ($Q_{2_1^+}$) of the first excited 2^+ state for even calcium isotopes.

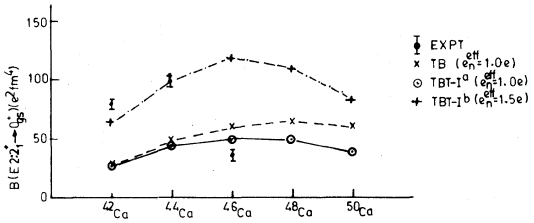

FIG. 8. The $B(E2{:}2_1^+ \rightarrow 0_{g.s.}^+)$ for even calcium isotopes.

$B(E2{:}2_1^+ \rightarrow 0_{g.s.}^+)$ values for ^{42,44}Ca are found to be very close to the corresponding experimental points, while there is a considerable deviation in the case of ^{46}Ca. This particular difference may be due to the near shell closure effects.

The quadrupole moments of the 2_1^+ state and the $B(E2)$ values for the transition $2_1^+ \rightarrow 0_{g.s.}^+$ for the lighter isotopes of Ca are close to the corresponding SM values and can reproduce the experimental values reasonably well with a proper choice of the effective charge. For the transitions involving the higher excited states, the calculated values are smaller as compared to the experiment. This is expected to be due to the neglect of the collective effects and to the use of the restricted space.

2. $N=28$ *isotones*

The $B(E2)$ values for the transitions $2_1^+ \rightarrow 0_{g.s.}^+$, $4_1^+ \rightarrow 2_1^+$, and $6_1^+ \rightarrow 4_1^+$ values for ^{50}Ti, ^{52}Cr, and ^{54}Fe are tabulated in Table IV. The $B(E2{:}2_1^+ \rightarrow 0_{g.s.}^+)$ values for all the three isotones are plotted in Fig. 9. The calculated and observed $Q_{2_1^+}$ values are shown in Fig. 10. All the calculated results are presented by using a single effective proton charge $e_p^{\text{eff}} = 1.5e$.

Inspection of Table IV reveals that the experimental $B(E2)$ values are well reproduced (within a factor of 2), except for $4_1^+ \rightarrow 2_1^+$ and $6_1^+ \rightarrow 4_1^+$ transitions in ^{52}Cr. These departures may be attributed to the core excitations not included in the calculation. Figure 9 demonstrates that the observed variation of the $B(E2{:}2_1^+ \rightarrow 0_{g.s.}^+)$ with the mass number is indeed well reproduced by the calculation.

The BPA results for these $N=28$ isotones reflect that (i) the neutron excitation from the $f_{7/2}$ orbit, (ii) the collective excitations, and (iii) the $\nu \geq 4$ and higher excited configurations, not included in the BPA calculation, are important and should be taken into account for a better description of the nuclear properties for these nuclei.

C. Energy spectra of even isotopes of Ti, Cr, and Fe

Shell model calculations with realistic interactions have not been reported so far for the f-p shell nuclei having both types of valence nucleons, except that for ^{44}Ti (Refs. 5, 23, and 27) using the Kuo-Brown and the modified Kuo-Brown interaction matrix elements. An obvious reason appears to be due to the practical difficulties encountered in handling the prohibitively large Hamiltonian matrices. Some calculations for $N \sim 28$ nuclei have recently been attempted[37,38] in the framework of the phenomenological shell model by considering either a pure $f_{7/2}$ model space or by allowing a restricted number of excitations from the $f_{7/2}$ orbit to the $p_{3/2}$ orbit, but no consistent picture has so far emerged from these analyses.

The BPA calculations for all these isotopes can be performed in the full f-p space as the maximum dimensionality of the energy matrices encountered in the present calculations corresponds to that of the shell model for ^{44}Ti. However, encouraged by the success of the projection method which adequately incorporates the effects of the space trunca-

TABLE IV. The experimental and the calculated $B(E2{:}J_i \rightarrow J_f)$ for $N=28$ isotones (with respect to ^{48}Ca core).

Nucleus	Transition $J_i \rightarrow J_f$	$B(E2)(e^2\text{fm}^4)$ TB[a]	expt	Reference[b]
^{50}Ti	$2_1^+ \rightarrow 0_{g.s.}^+$	58	66 ± 8	30, 33
	$4_1^+ \rightarrow 2_1^+$	59	60 ±12	30
	$6_1^+ \rightarrow 4_1$	30	34.2± 1.2	30
^{52}Cr	$2_1^+ \rightarrow 0_{g.s.}^+$	86	132 ± 6	34
	$4_1^+ \rightarrow 2_1^+$	0.76	79 ±17	35
	$6_1^+ \rightarrow 4_1^+$	0.18	59.5± 3.4	30, 35
^{54}Fe	$2_1^+ \rightarrow 0_{g.s.}^+$	81	108 ±10	36
	$4_1^+ \rightarrow 2_1^+$	36	78 ±16	30, 35
	$6_1^+ \rightarrow 4_1^+$	20	40 ± 0.5	30, 35

[a] $e_p^{\text{eff}} = 1.5e$.

[b] Reference to experimental data.

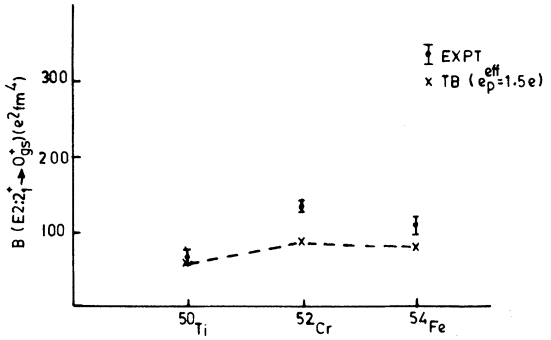

FIG. 9. The $B(E2{:}2_1^+ \rightarrow 0_{g.s.}^+)$ for $N=28$ isotones w.r.t. ^{48}Ca core.

tion as shown in the case of Ca isotopes, we, as a first step, perform the BPA calculations in the truncated space(s) only.

The Tabakin interaction matrix elements with respect to the ^{40}Ca core are appropriately renormalized for each of the truncated spaces I ($f_{7/2}-p_{3/2}$) and II ($f_{7/2}$) by the projection method to take into account the effects of the space truncation. The renormalized matrix elements thus obtained are then used in the BPA calculations. The Kuo-Brown SPE used in the present calculation are the same as those used for Ca isotopes.

The calculated excitation energies for 0^+, 2^+, 4^+, and 6^+ states for all the isotopes under consideration are shown in Figs. 11–14.

In order to analyze the effects of modification in the interaction matrix elements on the calculated spectra, the GBPA calculations are repeated for $N=26$ and $N=28$ nuclei using the modified and then renormalized (by the projection method to include the space truncation effects) set of Tabakin matrix elements. The results obtained by using

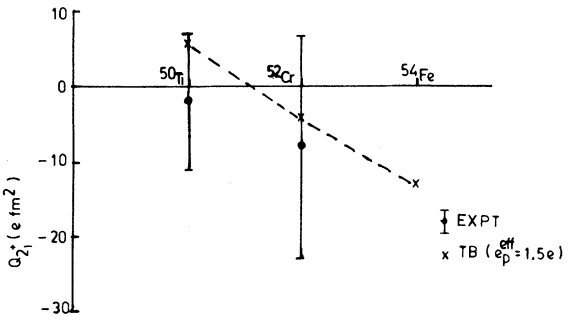

FIG. 10. The $Q_{2_1^+}$ for $N=28$ isotones w.r.t. ^{48}Ca core. expt corresponds to Ref. 33 for Ti and Ref. 23 for Cr.

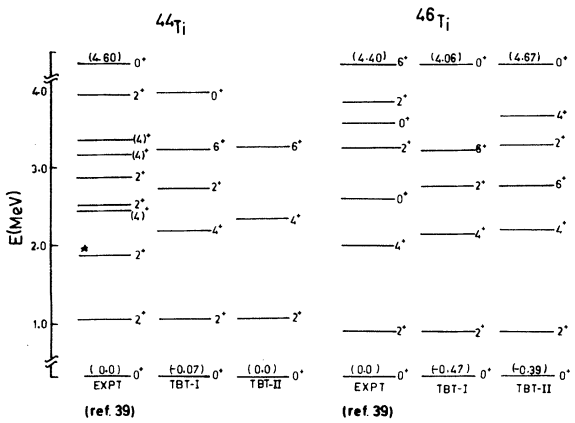

FIG. 11. The experimental (expt) and the GBPA energy spectra with shift for ^{44,46}Ti. For details see caption for Fig. 1.

these modified matrix elements are also included (labeled MTBT I) in the respective figures.

1. *Titanium isotopes*

The calculated and observed excitation energies for ^{44,46,48,50}Ti are shown in Figs. 11 and 12. Inspection of Fig. 11 reveals that the low lying states of ^{44}Ti, in comparison with the experiment, are well reproduced by the BPA in spite of the fact that the BPA calculations are carried out in the truncated space(s). Furthermore, our results compare equally well with the corresponding SM results[5,27] obtained in the full f-p space using the Kuo-Brown interaction matrix elements.

The experiment levels of ^{44}Ti quoted by Bhatt

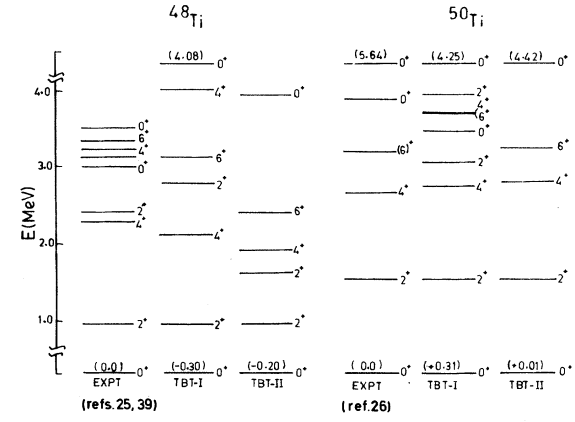

FIG. 12. The experimental and the GBPA energy spectra with shift for ^{48,50}Ti. For details see caption for Fig. 1.

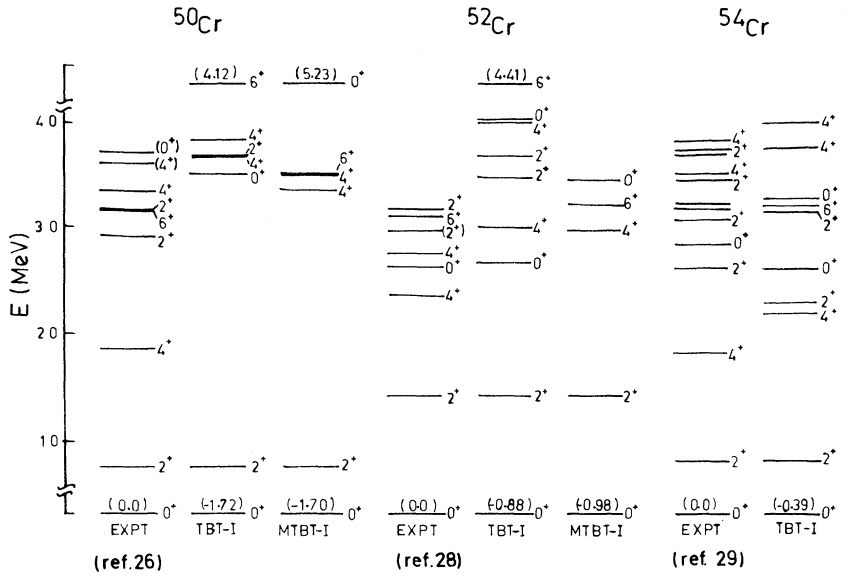

FIG. 13. The experimental and the GBPA energy spectra with shift for even Cr isotopes. For details see caption for Fig. 1.

and McGrory[27] are due to Rapaport *et al.*[42] who identify the state observed at 1.90 MeV as a 0^+ state. Later experiments of Baer *et al.*[39] have shown that the state observed at 1.89 MeV (corresponding to the 1.90 MeV 0^+ state of Rapaport *et al.*[42]) is a 2^+ state and not a 0^+ state. However, neither the shell model nor the BPA has been able to reproduce this state. Bhatt and McGrory,[27] considering this state as an observed 0^+ state, interpret it as a deformed state obtained from the admixture of an excited 0^+ state[43] of ^{40}Ca (which is assumed to be the core) with the ground state of ^{44}Ti. Along similar lines, the 2^+ state observed at 1.89 MeV may be interpreted as a deformed state obtained by the admixture of a core (^{40}Ca) excited 2^+ state with the ground state of ^{44}Ti. This interpretation seems to be quite reasonable if one recalls that such core excited deformed states are present even in the observed spectra of ^{42}Ca and ^{44}Ca.

Results in only $f_{7/2}$ space (TBT II) are satisfac-

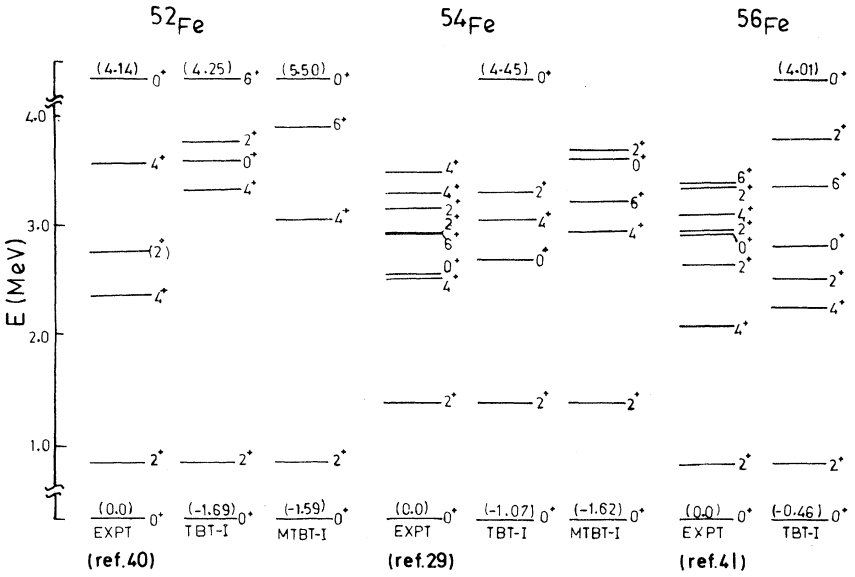

FIG. 14. The experimental and the GBPA energy spectra with shift for even Fe isotopes. For details see caption for Fig. 1.

tory for the first even-parity spin states. This indicates that for explaining the full spectrum, at least the excitations from $f_{7/2}$ to $p_{3/2}$ should be included in the calculation.

The calculated energy levels of ^{46,48,50}Ti shown in Figs. 11—13 along with the corresponding observed levels exhibit a similar trend, as is shown by the levels of ^{44}Ti. The first excited 0^+ states observed at 2.61 MeV ^{46}Ti and 3.0 MeV for ^{48}Ti not reproduced by the calculation perhaps are the deformed core (^{40}Ca) excited 0^+ states built on the ground states of ^{46}Ti and ^{48}Ti, respectively. For ^{50}Ti some additional levels near 3 MeV, which do not have any experimental correspondence, do appear in the TBT I spectrum. For this isotope, being a shell closure nucleus, we have repeated the BPA calculations in the truncated space I using the modified matrix elements. This improves the results in the sense that the additional levels which appear in the TBT I spectrum as mentioned above now disappear from the calculated spectrum. This is quite clear from the MTBT I spectrum shown in Fig. 12. Furthermore, the comparison of TBT I and MTBT I spectra (Fig. 12) with the TB spectrum of ^{50}Ti (Fig. 6) clearly shows the importance of the neutron excitations not considered in the BPA calculation (^{50}Ti) where ^{48}Ca is assumed to be an inert core.

2. *Chromium isotopes*

The calculated and experimental excitation energies for ^{50,52,54}Cr are plotted in Fig. 13. For Cr isotopes there are four valence protons and more than four valence neutrons distributed in the *f-p* shell. This means that the seniority four configurations of protons as well as of neutrons, not included in the present calculations, may play an important role. Similar remarks hold for Fe isotopes. Therefore, one may not expect good results for all the levels of these isotopes, especially for the case of ^{50}Cr and ^{52}Fe, where the excitations of the six valence neutrons will be considerably affected by near shell closure effects of $f_{7/2}$ neutron orbit. [These effects are indeed reflected in the calculated spectrum (TBT I) of ^{50}Cr and ^{52}Fe shown in Figs. 13 and 14, respectively]. Therefore, on an average we intend to investigate the qualitative trends only.

It is revealed in Fig. 13 that the low lying states 4^+ (1.88 MeV), 2^+ (2.92 MeV), and 6^+ (3.16 MeV) observed in the experimental spectrum of ^{50}Cr are absent in the calculated spectrum (TBT I). A similar observation holds for the results MTBT I. It is apparent from Fig. 13 that the shift in both the TBT I and the MTBT I spectra is of the same order (~ 1.7 MeV), which is significantly large. Clearly, the changes in the calculated spectrum caused by using the modified matrix elements cannot be regarded as an improvement in the results. Therefore, it appears that for this ($N=26$) nucleus in particular, the neglected configurations are important.

The excitation energies of ^{52}Cr, shown in Fig. 13, reveal that the BPA results (both TBT I and MTBT I) have been able to reproduce only the qualitative trend of the observed (expt) spectrum. The calculated levels in TBT I around 3 MeV, although not having one to one correspondence with the experimental levels, do exhibit a similar pattern as is observed in the experiment. This pattern is absent in the MTBT I spectrum.

For the case of ^{54}Cr, almost all the low lying levels (TBT I) shown in Fig. 13 have a good correspondence with the experimental levels. The calculated splitting between 4_1^+ and 2_2^+ is small as compared to the experimental splitting; otherwise the calculated spectrum is quite satisfactory. Corresponding to two unassigned levels around 3 MeV in the observed spectrum, we obtain a 6^+ and a 0^+ state.

3. *Iron isotopes*

The calculated and observed energies for these isotopes are shown in Fig. 14. The comparison of the calculated and observed spectra of ^{52}Fe shows a similar trend as that of ^{50}Cr. Both these nuclei have $N=26$. A similar trend is shown by the MTBT I results of ^{52}Fe.

For the case of ^{54}Fe, keeping in mind the effects of the shell closure for $N=28$ nuclei, the TBT I levels of this isotope shown in Fig. 14 are in reasonably good agreement with experiment. The states appearing around 3 MeV in the observed spectrum are absent in TBT I. These states may correspond to the configurations not included in the present calculation. The MTBT I results do not further improve the agreement.

Inspection of the results for ^{56}Fe (Fig. 14) reveals that almost all the calculated levels have a close resemblance with the corresponding observed levels and the relative excitation energies are very well reproduced.

To summarize the above results we state that the BPA has been able to reproduce the low lying experimental spectrum of even Ti isotopes reasonably

TABLE V. The BPA, the shell model, and the experimental $B(E2{:}J_i \rightarrow J_f)$ for even Ti isotopes. R_p (R_n) represents the individual proton (neutron) contribution.

Nucleus	Transition $J_i \rightarrow J_f$	R_p[a]	R_n[b]	$B(E2)$ (e^2fm^4) TBT I[c]	SM[e]	expt	Reference[d]
	$2_1^+ \rightarrow 0_{g.s.}^+$	10.54	10.62	140	116	120 ±30	44
						117 ±25	35
						157 ±22	30
^{44}Ti	$4_1^+ \rightarrow 2_1^+$	16.08	16.00	179	162	252 ±75	30, 35
						280 ±60	44, 35
	$6_1^+ \rightarrow 4_1^+$	18.24	18.24	160	139	157 ±22	30, 35
	$2_1^+ \rightarrow 0_{g.s.}^+$	−11.82	−10.28	157		160 ±34	24, 45
						171 ± 8	34
						209 ±12	35
						214 ±20	33
						217 ±17	46
^{46}Ti	$4_1^+ \rightarrow 2_1^+$	17.07	13.90	173		177 ±20	35, 46
	$6_1^+ \rightarrow 4_1^+$	17.42	16.29	138		150 ±80	35, 46
	$2_1^+ \rightarrow 0_{g.s.}^+$	11.97	10.49	162		151 ±18	36
						142 ± 8	35
						138 ±12	33
						140 ±28	45
						146 ±24	25
^{48}Ti	$4_1^+ \rightarrow 2_1^+$	17.18	13.22	169		35 ±22	35
	$6_1^+ \rightarrow 4_1^+$	−17.29	−16.58	139		53 ± 5	30, 35
	$2_1^+ \rightarrow 0_{g.s.}^+$	−11.97	−9.82	154		66 ± 8	30, 33, 35
						48 ± 4	47
						49 ± 8	36, 48
						63 ± 6	34
^{50}Ti	$4_1^+ \rightarrow 2_1^+$	17.17	12.05	159		60 ±12	30, 35
	$6_1^+ \rightarrow 4_1^+$	−16.92	−12.56	111		34.2± 1.2	30, 35

[a] $e_p^{\text{eff}} = e$.
[b] $e_n^{\text{eff}} = e$.
[c] $e_p^{\text{eff}} = 1.5e$ and $e_n^{\text{eff}} = 1.0e$.
[d] Reference to experimental data.
[e] Reference 27.

well. For the even isotopes of Cr and Fe, the BPA results do exhibit the observed trend, even the low lying spectra of ^{54}Cr and ^{56}Fe are in good agreement with the experiment. Considering the fact that no systematic microscopic calculations for these nuclei have been reported so far, the results of the BPA calculation without any adjustable parameter, presented here can be considered to be satisfactory. However, certain departures from the experimental trends are observed for nuclei having $N = 26$ or 28. This reflects the importance of the shell closure effects. The results with the use of modified matrix elements do not further improve the calculated trends. This shows that to incorporate the shell closure effects, the modification[5] of the matrix elements is not a solution. In addition, the Tabakin interaction matrix elements as they are, may not be most suitable in reproducing the experimental data quantitatively. The collective excitations and the higher seniority configurations, neglected in the present calculation, seem to be important especially for the nuclei with large ($N \geq 4$) number of valence particles of each type.

D. $E2$ transition and quadrupole moments for even Ti, Cr, and Fe isotopes

The individual proton and neutron contributions to the reduced transition matrix elements with

TABLE VI. The BPA and the experimental quadrupole moment ($Q_{2_1^+}$) of the first excited 2^+ state for even Ti isotopes.

Nucleus	$Q_{2_1^+}$ (e fm^2) Q_p[a]	Q_n[b]	TBT I[c]	expt	Reference[d]
^{44}Ti	−0.80	−0.80	−7.60		
^{46}Ti	−1.38	−1.09	−11.98	−19 ±10	32
				−21 ± 6	34
^{48}Ti	−1.56	−1.04	−12.79	−13.5± 8.8	49
				−15 ± 8	32
				−22 ± 8	33
^{50}Ti	−1.24	−0.01	−7.02	−2 ± 9	32
				8±16	34

[a] $e_p^{\text{eff}}=e$.
[b] $e_n^{\text{eff}}=e$.
[c] $e_p^{\text{eff}}=1.5e$ and $e_n^{\text{eff}}=1.0e$.
[d] Reference to experimental data.

$e_p^{\text{eff}}=e$ and $e_n^{\text{eff}}=e$ are given in Tables V, VII, and IX, and are labeled R_p and R_n, respectively. Similarly, the proton and the neutron contributions (Q_p and Q_n) to $Q_{2_1^+}$ are also presented in Tables VI, VIII, and X. However, the results with a single neutron effective charge $1.0e$ and a single proton effective charge $1.5e$, labeled TBT I, are also included in the respective tables along with the cor-

TABLE VII. The BPA and the experimental $B(E2{:}J_i\to J_f)$ for even Cr isotopes. R_p (R_n) represent the individual proton (neutron) contribution.

Nucleus	Transition $J_i\to J_f$	R_p[a]	R_n[b]	$B(E2)$ (e^2fm^4) TBT I[c]	expt	Reference[d]
	$2_1^+\to 0^+_{\text{g.s.}}$	−11.98	−12.32	183	208 ±23	46, 50−52
					204 ±34	34
					213 ±12	35
					227 ±20	30
					229 ±12	46
^{50}Cr	$4_1^+\to 2_1^+$	−13.76	−14.26	135	160 ±20	35, 46
	$6_1^+\to 4_1^+$	−7.96	−8.17	31	130 ±30	35, 46
	$2_1^+\to 0^+_{\text{g.s.}}$	12.24	12.08	185	132 ± 6	34
					96 ± 4	47
					119 ± 7	52
					115 ± 7	35
					113 ±10	36, 53
^{52}Cr	$4_1^+\to 2_1^+$	−15.95	1.04	58	79 ±17	35
					83 ±17	30
	$6_1^+\to 4_1^+$	−9.89	−11.61	54	59.5± 3.4	30, 35
	$2_1^+\to 0^+_{\text{g.s.}}$	9.07	12.56	137	200 ±14	32
^{54}Cr	$4_1^+\to 2_1^+$	−11.63	−17.99	139		
	$6_1^+\to 4_1^+$	11.64	17.77	95		

[a] $e_p^{\text{eff}}=e$.
[b] $e_n^{\text{eff}}=e$.
[c] $e_p^{\text{eff}}=1.5e$ and $e_n^{\text{eff}}=1.0e$.
[d] Reference to experimental data.

TABLE VIII. The BPA and the experimental quadrupole moment ($Q_{2_1^+}$) of the first excited 2^+ state for even Cr isotopes.

Nucleus	$Q_{2_1^+}$ (e fm^2) Q_p[a]	Q_n[b]	TBT I[c]	expt	Reference[d]
^{50}Cr	−1.53	−1.43	−14.10	−30± 9	32
^{52}Cr	−1.21	0.04	−6.70	−8±15	32
^{34}Cr	−0.15	1.72	5.62	−11±13	32

[a] $e_p^{\text{eff}}=e$.
[b] $e_n^{\text{eff}}=e$.
[c] $e_p^{\text{eff}}=1.5e$ and $e_n^{\text{eff}}=1.0e$.
[d] Reference to experimental data.

responding observed (expt) values.

The shell model $B(E2)$ values have been reported only for ^{44}Ti by Bhatt and McGrory[27] and are included in Table V in the column labeled SM for comparison. In all these tables the $B(E2)$ values are given in units of e^2fm^4 and the $Q_{2_1^+}$ values in units of e fm^2.

It is observed from Table V that the proton and the neutron contributions (R_p and R_n) to the $E2$ transition have the same sign and are almost of the same order. It is further revealed in the same table that the overall agreement between the calculated (TBT I) and the observed $B(E2)$ values is quite good. For ^{44}Ti the calculated values TBT I are quite close to the corresponding shell model values. It is to be noted that for ^{44}Ti the BPA is identical to the shell model. Therefore, the close agreement obtained as mentioned above indicates that the Tabakin interaction is equally successful in reproducing the $B(E2)$ values. All the calculated $B(E2)$ values for ^{46}Ti are very close to the corresponding experimental values. The $B(E2{:}2_1^+\rightarrow 0_{\text{g.s.}}^+)$ for ^{48}Ti is very well reproduced, while for the remaining transitions in ^{48}Ti as well as in ^{50}Ti, the $B(E2)$ values are found to be larger than the corresponding experimental values by a factor ranging from

TABLE IX. The BPA, the shell model, and the experimental $B(E2{:}J_i\rightarrow J_f)$ for even Fe isotopes. R_p (R_n) represents the individual proton (neutron) contribution.

Nucleus	Transition $J_i\rightarrow J_f$	$B(E2)$ (e^2fm^4) R_p[a]	R_n[b]	TBT I[c]	expt	Reference[d]
	$2_1^+\rightarrow 0_{\text{g.s.}}^+$	−11.90	−11.89	177		
^{52}Fe	$4_1^+\rightarrow 2_1^+$	12.48	12.46	108		
	$6_1^+\rightarrow 4_1^+$	−9.49	−9.51	43		
	$2_1^+\rightarrow 0_{\text{g.s.}}^+$	−12.14	−12.08	184	108±10	36
					122	48
					102± 4	47
^{54}Fe	$4_1^+\rightarrow 2_1^+$	−2.93	−3.56	7	78±16	30, 35
					≤147	48
	$6_1^+\rightarrow 4_1^+$	10.81	11.65	59	40± 0.5	30, 35
	$2_1^+\rightarrow 0_{\text{g.s.}}^+$	8.98	12.56	135	194± 4	32
56Fe	$4_1^+\rightarrow 2_1^+$	−11.77	−17.91	140		
	$6_1^+\rightarrow 4_1^+$	−12.47	−17.94	103		

[a] $e_p^{\text{eff}}=e$.
[b] $e_n^{\text{eff}}=e$.
[c] $e_p^{\text{eff}}=1.5e$ and $e_n^{\text{eff}}=1.0e$.
[d] Reference to experimental data.

TABLE X. The BPA and the experimental quadrupole moment ($Q_{2_1^+}$) of the first excited 2^+ state for even Fe isotopes.

Nucleus	$Q_{2_1^+}$ (e fm^2) Q_p[a]	Q_n[b]	TBT I[c]	expt	Reference[d]
^{52}Fe	−1.40	−1.40	−13.26		
^{54}Fe	−0.83	0.08	−4.41		
^{56}Fe	0.18	1.77	7.71	−24±3	32

[a] $e_p^{\text{eff}}=e$.
[b] $e_n^{\text{eff}}=e$.
[c] $e_p^{\text{eff}}=1.5e$ and $e_n^{\text{eff}}=1.0e$.
[d] Reference to experimental data.

$\sim 2-3$. As these nuclei have 26 and 28 neutrons, respectively, these deviations might be due to the shell closure effects. Recalling that the $B(E2)$ values for all the transitions in ^{50}Ti with respect to the ^{48}Ca core presented earlier in Table IV, are in fair agreement with the experiment, the comparison of the BPA result (TBT I) for ^{50}Ti with respect to the ^{40}Ca core (Table V) and the BPA result (TB) with respect to the ^{48}Ca core (Table IV) helps in realizing the effects of $f_{7/2}$ shell closure. The variation of $B(E2{:}2_1^+\rightarrow 0_{\text{g.s.}}^+)$ with mass number for Ti isotopes is in fair agreement with the experiment. However, for ^{50}Ti the calculated value is larger by a factor of 3. The shell closure effects may be responsible for this departure as mentioned earlier. The experimental trend of the variation of $Q_{2_1^+}$ with the mass number for these isotopes is well reproduced.

The results for the Cr isotopes are given in Tables VII and VIII. Table VII reveals that the proton and the neutron contributions (R_p and R_n) are of the same order for all the transitions in Cr isotopes except for the transition $4_1^+\rightarrow 2_1^+$ in ^{52}Cr. This implies that the nuetron contributions are significant.

The trend of the variation of $B(E2{:}2_1^+\rightarrow 0_{\text{g.s.}}^+)$ with the mass number for Cr isotopes is reasonably close to the corresponding experimental values. For Cr isotopes the calculated and the observed $Q_{2_1^+}$ values are listed in Table VIII. Considering the large uncertainties observed in the experimental data for these isotopes, it is difficult to ascertain the quality of agreement between the calculated and observed values.

The $B(E2)$ values for Fe isotopes are presented in Table IX. The calculated values are in fairly good agreement with available observed values except for the transition $4_1^+\rightarrow 2_1^+$. This departure is due to the smaller values of R_p and R_n, indicating that there are cancellation effects within the proton (neutron) contributions. The variation of the $B(E2{:}2_1^+\rightarrow 0_{\text{g.s.}}^+)$ with the mass number for the Fe isotopes though different from experiment, is similar to the one for Cr isotopes. Similarly, the $Q_{2_1^+}$ values for Fe isotopes exhibit a trend resembling that for the Cr isotopes.

We summarize the results for Ti, Cr, and Fe isotopes by stating that the overall agreement between the calculated and observed $B(E2)$ as well as $Q_{2_1^+}$ values is fairly good. Some departures from the experiment have been found only in few cases where either the individual proton (R_p) and/or neutron (R_n) contributions are small, or the nuclei have $N=26$ or 28 for which the shell closure effects are important. The BPA results are also in good agreement with the corresponding shell model results which are available only for ^{44}Ti. The variation of the calculated $B(E2{:}2_1^+\rightarrow 0_{\text{g.s.}}^+)$ with the mass number; for the isotopes of Ti, Cr, and Fe, exhibits almost the same trend i.e., the $B(E2{:}2_1^+\rightarrow 0_{\text{g.s.}}^+)$ value initially increases with the mass number, attains a maximum, and then starts decreasing with a further increase in the mass number. Although, for Cr and Fe isotopes, the calculation does not reproduce the observed trend, the calculated values are reasonably close to the corresponding observed values.

In general, the wave functions obtained from the BPA energy calculations are able to reproduce reasonably well most of the observed $E2$ transitions and the quadrupole moments of the first excited 2^+ state.

IV. CONCLUSIONS

A close agreement between the BPA and the available shell model results clearly demonstrates

the validity of the BPA as a reasonable approximation to the seniority (or exact) shell model in this region. This in turn suggests that the BPA which involves small dimensions (≤ 4 particle shell model), can be applied in practice to almost all the cases and therefore, it can be regarded as a viable alternative to the seniority (or exact) shell model.

It is shown that the projection method employed here successfully incorporates the effects of truncation of the valence levels through the renormalization of the two body interaction matrix elements. This indicates that the many body effects, introduced due to the truncation of valence levels, are small, especially for a small number of valence nucleons compared to the total occupancy of the truncated valence space. Therefore, these renormalized matrix elements can be employed with confidence for the nuclear structure calculation in the truncated space(s).

The Tabakin interaction matrix element, used in the present analysis, have been able to reproduce the available shell model results for Ca isotopes and for ^{44}Ti. In addition, the general observed trends are well predicted by the use of these matrix elements. Our results demonstrate an overall good agreement with the experiment. The maximum differences arise for the nuclei having $N=26$ or 28. These may be attributed to the $f_{7/2}$ shell closure effects not included appropriately in the calculated Tabakin as well as in the Kuo-Brown interaction matrix elements. The modification in the $T=1$ matrix element proposed by McGrory *et al.*[4] does not seem to help in further improving the results. The problem still remains for obtaining the correct set of matrix elements for this region incorporating the proper shell closure effects.

It is felt that in order to further improve the quantitative agreement with the experiment for the higher states of the $2p$-$1f$ shell nuclei, the calculation should be extended to take into account the collective excitations (core excitations) and the higher seniority configurations not included in the present calculation.

ACKNOWLEDGMENTS

We are thankful to H. J. Mang, P. Ring, P. P. Kane, S. H. Patil, V. L. Narasimham, and G. Basavaraju for their continuous interest in this work. One of us (S.H.) is thankful to the C. S. I. R. (India) for partial financial support. The help rendered by the Computer Centre, I. I. T. Bombay, is gratefully acknowledged. This work was supported in part by the Bundesministerium für Forschung und Technologie.

*Present address: Department of Physics, Technische Universität München, D 8046 Garching, West Germany.

[1]*Proceedings of the Topical Conference on the Structure of $1f_{7/2}$ Nuclei, Padua, Italy, 1971,* edited by R. A. Ricci (Editrice Compositori, Bologna, 1971); K. Allart, K. Goeke, H. Muther and A. Faessler, Phys. Rev. C 9, 988 (1974) and references therein; A. K. Dhar and K. H. Bhatt, *ibid.* 16, 792 (1977); 14, 1630 (1976); Nucl. Phys. A285, 93 (1977) and references therein; S. Saini and M. R. Guney, J. Phys. G 4, 219 (1978).

[2]I. Talmi, Rev. Mod. Phys. 34, 704 (1962); J. D. McCullen, B. F. Bayman, and L. Zamick, Phys. Rev. 134, B515 (1964); J. N. Ginocchio and J. B. French, Phys. Lett. 7, 137 (1963); R. D. Lawson, Nucl. Phys. A173, 17 (1971) and references therein.

[3]B. J. Raz and M. Soga, Phys. Rev. Lett. 24, 924 (1965); T. Engeland and E. Osnes, Phys. Lett. 20, 424 (1966).

[4]J. B. McGrory, B. H. Wildenthal, and E. C. Halbert, Phys. Rev. C 2, 186 (1970).

[5]J. B. McGrory, Phys. Rev. C 8, 693 (1973).

[6]T. T. S. Kuo and G. E. Brown, Nucl. Phys. A114, 241 (1968).

[7]M. H. Macfarlane, in *Lectures in Theoretical Physics,* edited by P. D. Kunz and W. E. Britin (University of Colorado Press, Boulder, Colorado, 1966), Vol. VIII C, p. 583 and references therein; Y. K. Gambhir and Ram Raj, Phys. Rev. 161, 1125 (1967).

[8]P. L. Ottaviani and M. Savoia, Phys. Rev. 178, 1594 (1969); 187, 1306 (1969); Lett. Nuovo Cimento 1, 766 (1969); Nuovo Cimento 67, 630 (1970).

[9]Y. K. Gambhir, A. Rimini, and T. Weber, Phys. Rev. 188, 1573 (1969); Phys. Rev. C 3, 1965 (1971).

[10]B. Lorazo, Phys. Lett. 29B, 150 (1969); Nucl. Phys. A153, 255 (1970); K. Allart and E. Boeker, *ibid.* A168, 630 (1971); A198, 33 (1972); S. Haq and Y. K. Gambhir, Phys. Rev. C 16, 2455 (1977); Y. K. Gambhir, S. Haq, and J. K. Suri, *ibid.* 20, 381 (1979); 21, 1124 (1980) and Ann. Phys. (N.Y.) 133, 154 (1981).

[11]B. R. Mottelson, Probleme a N Corps, Les Houches, 1958 (unpublished).

[12]M. Harvey and T. Sabe, Atomic Energy of Canada Ltd., Report AECL 3007, 1968.

[13]B. R. Barret, E. C. Halbert, and J. B. McGrory, Ann. Phys. (N.Y.) 90, 321 (1975).

[14]Y. K. Gambhir and G. Basavaraju, Pramāna 13, 47

(1979).
[15]A. Rimini and T. Weber, Phys. Rev. C 2, 324 (1970).
[16]A. R. Edmonds, *Angular Momentum in Quantum Mechanics* (Princeton University Press, Princeton, New Jersey, 1957).
[17]T. Hamada and J. D. Johnston, Nucl. Phys. 34, 382 (1962).
[18]Y. K. Gambhir (unpublished).
[19]F. Tabakin, Ann. Phys. (N.Y.) 30, 51 (1964).
[20]A. K. Kerman and M. K. Pal, Phys. Rev. 162, 970 (1967).
[21]D. M. Clement and E. U. Baranger, Nucl. Phys. A108, 27 (1968).
[22]T. A. Belote, A. Sperduto, and W. E. Buechner, Phys. Rev. 139, 80 (1965).
[23]P. M. Endt and C. Van Der Leun, Nucl. Phys. A214, 490 (1973); A214, 534 (1973).
[24]R. L. Auble, Nucl. Data B4, 269 (1970).
[25]J. Rapaport, Nucl. Data B4, 351 (1970).
[26]Nucl. Data Sheets 19, 291 (1976).
[27]K. H. Bhatt and J. B. McGrory, Phys. Rev. C 3, 2293 (1971).
[28]Nucl. Data Sheets 25, 235 (1978).
[29]H. Verheul, Nucl. Data B3-5, 6 (1970).
[30]B. A. Brown, D. B. Fossan, J. M. McDonald, and K. A. Snover, Phys. Rev. C 9, 1033 (1974).
[31]J. D. McCallen and D. J. Donahue, Phys. Rev. C 8, 1406 (1973).
[32]Nucl. Data Tables 11, 281 (1973).
[33]O. Haüsser, D. Pelte, T. K. Alexander, and H. C. Evans, Nucl. Phys. A150, 417 (1970).
[34]C. W. Towsley, D. Cline, and R. N. Horoshko, Nucl. Phys. A250, 381 (1975).
[35]W. Kutschera, quoted in Ref. 1 [Phys. Rev. C 16, 792 (1977)] as private communication.
[36]W. Kutschera, R. B. Huber, C. Signorini, and P. Blasi, Nucl. Phys. A210, 531 (1973).
[37]A. Yokoyama, T. Oda, and H. Horie, Prog. Theor. Phys. 60, 427 (1978).
[38]D. S. Chuu, C. S. Han, M. C. Wang, and S. T. Hsieh, J. Phys. G 5, 59 (1978).
[39]H. W. Baer, J. J. Kraushaar, C. E. Moss, N. S. P. King, R. E. L. Green, P. D. Kunz, and E. Rost, Ann. Phys. (N.Y.) 76, 437 (1973).
[40]P. Decowski, W. Benenson, B. A. Brown, and H. Nann, Nucl. Phys. A302, 186 (1978).
[41]Nucl. Data Sheets 20, 253 (1977).
[42]J. Rapaport, J. B. Ball, R. L. Auble, T. A. Belote, and W. A. Dorenbusch, Phys. Rev. C 5, 453 (1972).
[43]M. A. Grace and A. R. Poletti, Nucl. Phys. 78, 273 (1966).
[44]W. R. Dixon, R. S. Storey, and J. J. Simpson, Nucl. Phys. A202, 579 (1973).
[45]P. H. Stelson and L. Grodzin, Nucl. Data A1, 2 (1965).
[46]W. Dehndardt, O. C. Kistner, W. Kutschera, and H. J. Sann, Phys. Rev. C 7, 1471 (1973).
[47]J. J. Simpson, J. A. Cookson, D. Eccleshall, and M. J. L. Yates, Nucl. Phys. 62, 385 (1965).
[48]O. F. Afonin, A. P. Grinberg, I. K. Lemberg, and I. N. Chugunov, Yad. Fiz. 6, 219 (1967) [Sov. J. Nucl. Phys. 6, 160 (1968)].
[49]P. M. S. Lesser, D. Cline, Ph. Goode, and R. N. Horoshko, Nucl. Phys. A190, 597 (1972).
[50]F. K. McGowan, P. H. Stelson, R. L. Robinson, W. J. Milner, and J. L. C. Ford Jr., in *Proceedings of the International Conference on Nuclear Spin-Parity Assignments* (Academic, New York, 1966), p. 222.
[51]S. Raman, R. L. Auble, W. T. Milner, J. B. Ball, F. K. McGowan, P. H. Stelson, and R. L. Robinson, Nucl. Phys. A184, 138 (1972).
[52]D. Cline, C. W. Towsley, and R. N. Horoshko, in *Proceedings of the International Conference on Nuclear Moments and Nuclear Structure, Osaka, Japan, 1972,* edited by H. Horie and K. Sugimoto [J. Phys. Soc. Jpn. Suppl. 34, 439 (1973)].
[53]J. Rapaport, Nucl. Data B3, 85 (1970).